

# A MOLECULAR DYNAMICS STUDY OF THE INFLUENCE OF CHEMICAL REDUCTION ON THE STRUCTURE OF AMORPHOUS GERMANIA

AGNIESZKA WITKOWSKA<sup>1,2</sup>, LEON MURAWSKI<sup>1</sup>  
AND GRZEGORZ BERGMAŃSKI<sup>3</sup>

<sup>1</sup>*Faculty of Technical Physics and Applied Mathematics,  
Technical University of Gdansk,  
Narutowicza 11/12, 80-952 Gdansk, Poland  
agnieszk@task.gda.pl*

<sup>2</sup>*TASK Computer Centre, Technical University of Gdansk,  
Narutowicza 11/12, 80-952 Gdansk, Poland*

<sup>3</sup>*Facoltà di Chimica, Università di Camerino,  
via Sant' Agostino 1, Camerino (MC), Italia*

(Received 20 October 2001)

**Abstract:** The contribution is dedicated to the molecular dynamics (MD) study of the structure of reduced germania glass of composition  $1\text{Ge } 1\text{GeO}_2$ . The work is inspired by a recent report on the formation of Ge clusters in hydrogen reduced germanate glasses containing oxides of heavy metals.

The MD simulations have been performed in the microcanonical (NVE) ensemble, using a simple two-body Born-Mayer-Huggins interaction potential.

A tendency of germanium atoms to agglomeration into clusters, observed in the present calculations, is compared with an analogous tendency of Bi and Pb atoms, observed previously in the  $x\text{Bi } (1-x)\text{GeO}_2$  and  $x\text{Pb } (1-x)\text{GeO}_2$  systems. The differences in the short and medium-range order in  $\text{GeO}_2$  system between the  $1\text{Ge } 1\text{GeO}_2$  and  $\text{GeO}_2$  glasses are discussed.

**Keywords:** oxide glasses, hydrogen reduction, molecular dynamics, structural modelling

## 1. Introduction

Germanate and silicate glasses containing oxides of heavy metals such as  $\text{PbO}$ ,  $\text{Bi}_2\text{O}_3$  or  $\text{Sb}_2\text{O}_3$  belong to a group of materials which on the high temperature annealing in hydrogen atmosphere undergo significant structural changes. In particular, at sufficiently high temperatures a certain number of hydrogen molecules (from the high-energy tail of the Maxwell-Boltzmann distribution) react with oxygen atoms of  $\text{GeO}_4$  or/and  $\text{SiO}_2$  tetrahedra, bonded simultaneously with metal ions. This chemical reaction results in the appearance of  $\text{H}_2\text{O}$  molecules. The  $\text{H}_2\text{O}$  molecules evaporate

from the glass, leading to a decrease of the sample mass. Simultaneously, the heavy metal ions become neutral atoms, which agglomerate into metal granules immersed in the germania or silica matrix. The changes of structural and other physical properties (*e.g.* surface conductivity) induced by high temperature annealing have been described in references [1–11].

Recently, in germanate glasses submitted to prolonged hydrogen annealing, in addition to metal granules also germanium clusters have been detected by X-ray diffraction methods [12]. The present simulation work is inspired by this new result. It is aimed to see whether and how the neutral germanium atoms agglomerate into clusters, and to compare qualitatively the agglomeration tendency of germanium with similar tendencies of heavy metal atoms. In particular, we describe the results of the molecular dynamics (MD) calculations of the structure of reduced amorphous germania of composition  $1\text{Ge } 1\text{GeO}_2$ , and compare it with the structure of pure amorphous  $\text{GeO}_2$  (*a*- $\text{GeO}_2$ ). Since rather qualitative and comparative results were expected, no effort has been done to reproduce perfectly high quality experimental structural data on *a*- $\text{GeO}_2$  or *a*-Ge. Such a work would require the usage of three body interactions, and their parametrisation was beyond the scope of the present work. Instead, we have chosen rather simple two-body interactions of the Born-Mayer-Huggins (BMH) form, given in [13]. The parametrisation of the Ge–O, Ge–Ge, and O–O interactions proposed in [13] allows one to reproduce well the main structural features of glassy germania [5, 14]. The main reason of our choice of the potential function in the BMH form was that our previous simulations of heavy atom agglomeration in germania matrix were performed also for the BMH interactions, so the comparison of the agglomeration tendencies in both materials becomes more straightforward.

The paper is organised as follows. In Section 2 we present in brief the simulation method. In Section 3 the tendency of Ge atoms to the agglomeration into granules is described. The differences in the short-range and medium-range order in the  $\text{GeO}_2$  phase between the  $1\text{Ge } 1\text{GeO}_2$  and  $\text{GeO}_2$  glasses are discussed in Sections 4 and 5, respectively. Section 6 contains concluding remarks.

## 2. Simulation method

The MD simulations (*e.g.* [15, 16]) have been performed in the microcanonical (NVE) ensemble. The two-body Born-Mayer-Huggins interaction potential has been applied, with the parametrisation proposed in [14]. The systems were initially prepared as well equilibrated hot melt, and then cooled down to the room temperature (the average cooling rate of  $2 \cdot 10^{13}$  K/s). The numbers of atoms within the simulation box and the box-edge lengths are given in Table 1. Usual periodic boundary conditions were applied.

**Table 1.** The numbers of atoms within the simulation box and the box-edge lengths

Glass composition	$\text{Ge}^{4+}$	$\text{Ge}^0$	$\text{O}^{2-}$	Box edge [ $\text{\AA}$ ]
$\text{GeO}_2$	500	—	1000	29.531
$1\text{Ge } 1\text{GeO}_2$	500	500	1000	34.33

The structural information on short-range correlations was obtained in a conventional way, mainly from pair and angular partial distribution functions (PDFs, and ADFs, respectively). The PDFs were approximated by  $\Gamma$ -like distributions in the following form [17, 18]:

$$g(r) = \frac{N}{4\pi\rho r^2} \frac{2}{\sigma \cdot |\beta| \cdot \Gamma(4/\beta^2)} \left( \frac{4}{\beta^2} + \frac{2(r-R)}{\sigma \cdot \beta} \right)^{\frac{4}{\beta^2}-1} \cdot \exp \left[ - \left( \frac{4}{\beta^2} + \frac{2(r-R)}{\sigma \cdot \beta} \right) \right], \quad (1)$$

where  $N$  is the co-ordination number,  $\rho$  is the density,  $R$  is the average distance,  $\sigma^2$  is the variance (Debye-Waller-like parameter),  $\beta$  is the asymmetry (skewness) parameter, and  $\Gamma(x)$  is the Euler's gamma function, calculated for  $x = 4/\beta^2$ . The latter formula is valid for  $(r-R)\beta > -2\sigma$ .

The medium-range order was studied via the cation-anion ring analysis, performed using our recent highly efficient redundancy aware algorithm [19, 20], implemented in the ANELLI programme package [21–23].

### 3. Spatial distributions of $\text{Ge}^{4+}$ ions and $\text{Ge}^0$ atoms

In Figure 1 we show the pair distribution functions that reveal the spatial arrangement of  $\text{Ge}^{4+}$  ions and  $\text{Ge}^0$  neutral atoms in the  $\text{GeO}_2$  and 1Ge 1GeO<sub>2</sub> systems.

The most probable  $\text{Ge}^{4+}$ – $\text{Ge}^{4+}$  distances are equal to 3.36 Å and to 3.32 Å in  $\text{GeO}_2$  and 1Ge 1GeO<sub>2</sub> systems, respectively. Moreover, the PDF peak in partially reduced glass is wider than in unreduced system. This means that the dispersion in the  $\text{Ge}^{4+}$ – $\text{Ge}^{4+}$  distances increases during the reduction, and so the germania subsystem becomes more disordered. The  $\text{Ge}^{4+}$ – $\text{Ge}^{4+}$  average co-ordination number in pure  $\text{GeO}_2$  equals to 4.02 (as read in the PDF minimum between the first two peaks, *i. e.* at 3.64 Å). Simultaneously, the average  $\text{Ge}^{4+}$ – $\text{Ge}^{4+}$  co-ordination number in 1Ge 1GeO<sub>2</sub>, as read in the PDF minimum between the first two peaks, *i. e.* at 3.60 Å, equals to about 4.08. The distributions of the co-ordinations numbers (in percent) in both compounds, calculated up to the mentioned before cut-off radii are given in Table 2. As one can see, although the average  $\text{Ge}^{4+}$ – $\text{Ge}^{4+}$  co-ordination numbers are rather similar, the distributions of individual numbers of the neighbours differ strongly. Since the  $\text{Ge}^{4+}$  ions are caged by oxygen ions (see Section 4), from the Table results that the germania network in 1Ge 1GeO<sub>2</sub> is more complicated and strained than in the  $\text{GeO}_2$  system.

The  $\text{Ge}^{4+}$ – $\text{Ge}^0$  pair correlation in 1Ge 1GeO<sub>2</sub> is also shown in Figure 1. As it is seen, the most probable  $\text{Ge}^{4+}$ – $\text{Ge}^0$  distance is very long (about 3.78 Å), the first peak height is hardly higher than one. The co-ordination number read at the distance of 5 Å amounts to about 3. Simultaneously, the  $\text{Ge}^0$ – $\text{Ge}^0$  co-ordination number read at the same distance of 5 Å, amounts to almost 10. This suggests a strongly non-uniform distribution of the neutral  $\text{Ge}^0$  atoms and the  $\text{Ge}^{4+}$  ions.

**Table 2.** Distributions [%] of the  $\text{Ge}^{4+}$ – $\text{Ge}^{4+}$  co-ordination numbers in  $\text{GeO}_2$  and 1Ge 1GeO<sub>2</sub> calculated up to the cut-off radii of 3.64 Å and 3.60 Å, respectively

Co-ordination	3-fold	4-fold	5-fold	6-fold	Average
$\text{GeO}_2$	0.6	96.8	2.6	—	4.021
1Ge 1GeO <sub>2</sub>	0.2	92.4	6.0	1.2	4.08

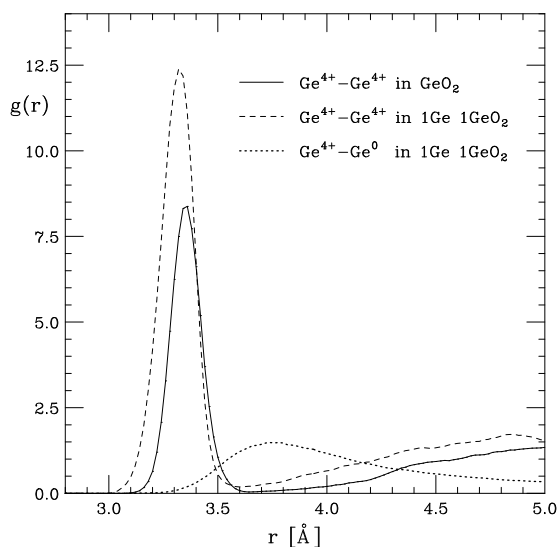


**Figure 1.** The  $\text{Ge}^{4+}\text{-Ge}^{4+}$  and  $\text{Ge}^{4+}\text{-Ge}^0$  pair distribution functions in the  $\text{GeO}_2$  and  $1\text{Ge } 1\text{GeO}_2$  systems

In Figure 2 (left panel) we show the configuration of all the atoms in the last simulation step of the  $1\text{Ge } 1\text{GeO}_2$  system. For clearer presentation the neutral  $\text{Ge}^0$  atoms are distinguished by larger ball radius. An agglomeration tendency is clearly seen. In Figure 2 (right panel) we show the  $\text{Ge}^0$  atoms only (at the same time-step as in Figure 2 (left panel)). Previously, a similar agglomeration tendency of heavy metal atoms, as Pb or Bi, has been observed in many completely reduced oxide systems [5, 7–10, 14]. Here, for comparison we cite our data on  $\text{Pb}^0$  atom agglomeration in the  $1\text{Pb } 1\text{GeO}_2$  system. The spatial distributions of all, and only  $\text{Pb}^0$  atoms in the last time step of a similar simulation performed for the  $1\text{Pb } 1\text{GeO}_2$  system are shown in Figure 3. The resulting configurations are qualitatively similar. In order to characterise the agglomeration tendencies quantitatively, we calculated the fractions of neutral atoms,  $\text{Ge}^0$  and  $\text{Pb}^0$ , respectively, of auto co-ordination higher or equal than  $n$ , where  $n$  is integer. The results are shown in Figure 4. As it is seen, the percentage of highly auto co-ordinated neutral atoms is higher in  $1\text{Ge } 1\text{GeO}_2$  than in  $1\text{Pb } 1\text{GeO}_2$  one. This means, that the  $\text{Ge}^0$  cluster has larger bulk to surface ratio than the  $\text{Pb}^0$ . In our simulations the cluster formation occurred at high temperatures, in the liquid state.

#### 4. Short range order in the $\text{GeO}_2$ subsystem

The best-fit parameters  $R$ ,  $\sigma^2$ ,  $\beta$ , and  $N$ , of the first PDF's peak, approximated by distribution (1), together with the most probable inter-atomic distances,  $R_o$ , *i.e.* the PDFs' maxima positions, for the  $\text{Ge}^{4+}\text{-O}^{2-}$  and  $\text{O}^{2-}\text{-O}^{2-}$  pairs are listed in Tables 3 and 4, respectively. The mentioned PDFs and the relevant angular distribution functions (ADFs) are shown in Figures 5 and 6, respectively.

The most probable  $\text{Ge}^{4+}\text{-O}^{2-}$  distances,  $R_0$ , are the same in both  $\text{GeO}_2$  and  $1\text{Ge } 1\text{GeO}_2$  systems up to  $0.01\text{Å}$ . Due to the peak asymmetry, the average distances,  $R$ , are slightly longer, and in our simulations amount to  $1.71\text{Å}$  in  $\text{GeO}_2$  and  $1.70\text{Å}$

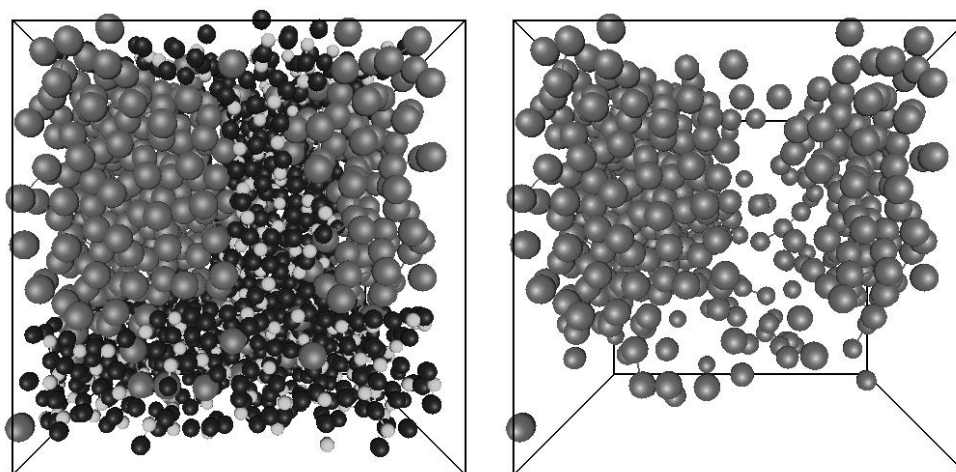


**Figure 2.** Spatial distributions of all the atoms (left panel) and neutral germanium atoms only (right panel) in the last simulation step of 1Ge 1GeO<sub>2</sub>. Large balls – Ge<sup>0</sup>, small light balls – Ge<sup>4+</sup>, small dark balls – O<sup>2-</sup>

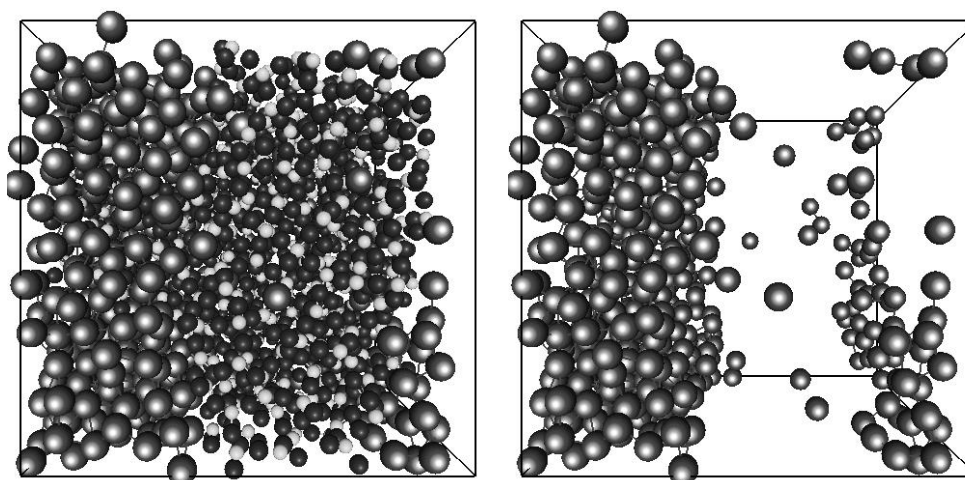


**Figure 3.** Spatial distributions of all the atoms (left panel) and neutral lead atoms only (right panel) in the last simulation step of 1Pb 1GeO<sub>2</sub>. Large balls – Pb<sup>0</sup>, small light balls – Ge<sup>4+</sup>, small dark balls – O<sup>2-</sup>

in 1Ge 1GeO<sub>2</sub>. The latter values are somewhat lower (by about 1%) than the Ge<sup>4+</sup>-O<sup>2-</sup> bond length reported in experimental works ( $1.74 \pm 0.02 \text{ \AA}$  in [24] or  $1.75 \text{ \AA}$  in [25, 26]). However, although the simulated Ge<sup>4+</sup>-O<sup>2-</sup> distances are slightly too short, the oxygen co-ordination of Ge<sup>4+</sup> ions determined experimentally has been fully reproduced in our calculations. Within the range of  $2.0 \text{ \AA}$  practically all the Ge<sup>4+</sup> cations have four oxygen neighbours (98.6% and 99.5% of the Ge<sup>4+</sup> cations in GeO<sub>2</sub> and 1Ge 1GeO<sub>2</sub>, respectively). The co-ordinations numbers read at the PDF minimum after the first peak, amount exactly to 4.0.

All the Ge<sup>4+</sup>O<sub>4</sub><sup>2-</sup> groups have tetrahedral symmetry, which follows from the inspection of the averaged angular O-Ge-O and O-O-O distributions, Figure 6, as

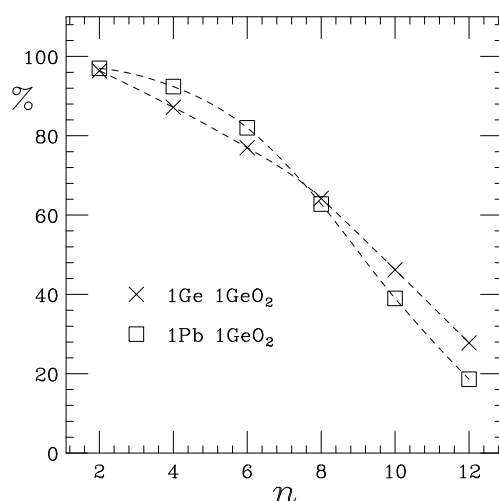


**Figure 4.** The fractions [%] of  $\text{Ge}^0$  and  $\text{Pb}^0$  atoms of auto-co-ordination higher than  $n$  in  $1\text{Ge } 1\text{GeO}_2$  and  $1\text{Pb } 1\text{GeO}_2$  systems

**Table 3.** The parameters  $R_o$ ,  $R$ ,  $\sigma^2$ ,  $\beta$ , and  $N$  for  $\text{Ge}^{4+}-\text{O}^{2-}$  correlations in  $\text{GeO}_2$  and  $1\text{Ge } 1\text{GeO}_2$

	$R_o$ [Å]	$R$ [Å]	$\sigma^2$ [Å <sup>2</sup> ]	$\beta$	$N$
$\text{GeO}_2$	1.70	1.71	0.002	0.30	3.931
$1\text{Ge } 1\text{GeO}_2$	1.69	1.70	0.002	0.25	3.95

**Table 4.** The parameters  $R_o$ ,  $R$ ,  $\sigma^2$ ,  $\beta$ , and  $N$  for  $\text{O}^{2-}-\text{O}^{2-}$  correlations in  $\text{GeO}_2$  and  $1\text{Ge } 1\text{GeO}_2$

	$R_o$ [Å]	$R$ [Å]	$\sigma^2$ [Å <sup>2</sup> ]	$\beta$	$N$
$\text{GeO}_2$	2.70	2.79	0.036	0.68	6.211
$1\text{Ge } 1\text{GeO}_2$	2.68	2.78	0.041	0.77	6.53

well as from the analysis of all individual local neighbourhoods of  $\text{Ge}^{4+}$  ions. Let us characterise the shape of the  $\text{Ge}^{4+}\text{O}^{2-}_4$  tetrahedra. The distributions of tetrahedrality parameters  $T_1$  [27] and  $T_2$  [28], defined as:

$$T_1 = \frac{\sum_i (l_{\text{O-O}} - l_{\text{O-O},i})^2}{l_{\text{O-O}}^2}, \quad (2)$$

$$T_2 = \frac{\sum_i (l_{\text{O-O}} - l_{\text{O-O},i})^2}{l_{\text{O-O}}^2} + \frac{\sum_i (l_{\text{Ge-O}} - l_{\text{Ge-O},i})^2}{l_{\text{Ge-O}}^2}, \quad (3)$$

have been calculated. In Equations (2) and (3)  $l_{\text{O-O},i}$  and  $l_{\text{Ge-O},i}$  are the lengths of the  $i^{\text{th}}$  tetrahedrons' O-O edge ( $i=1, \dots, 6$ ) and Ge-O distance ( $i=1, \dots, 4$ ), and  $l_{\text{O-O}}$  and  $l_{\text{Ge-O}}$  are the average O-O, and Ge-O distances, respectively. Shape parameters (2) and (3) are dimensionless, and being normalised to the average inter-atomic distances, characterise only the cation- $\text{O}_4$  groups geometry, and do not depend on particular values of bond lengths. The  $T_1$  parameter estimates only the overall shape of the tetrahedra, with no reference to the position of central cation, whereas the  $T_2$  estimator additionally takes into account deviations in the cation localisation. The ideal tetrahedron is characterised by zero-values of both estimators,  $T_1 = T_2 = 0$ .

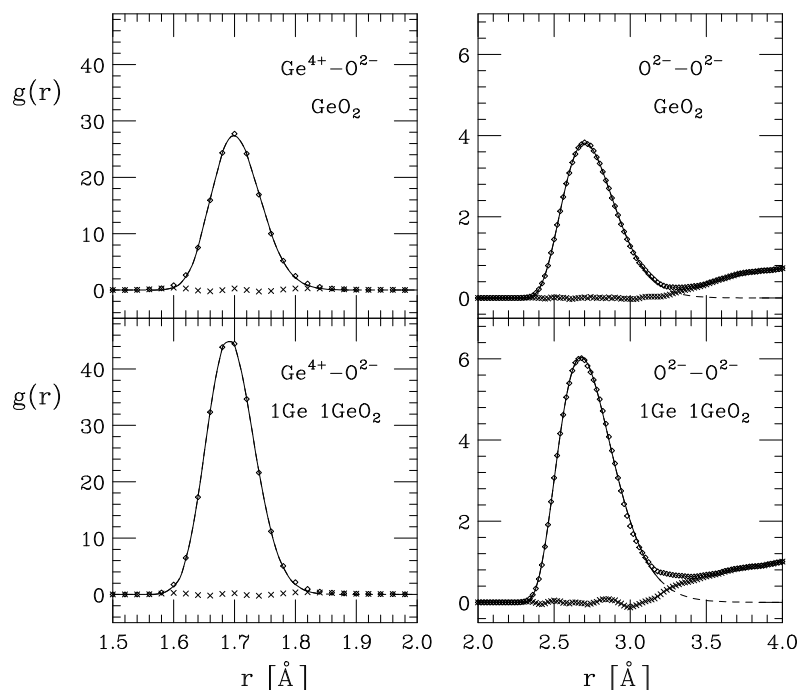


**Figure 5.** The  $\text{Ge}^{4+}-\text{O}^{2-}$  and  $\text{O}^{2-}-\text{O}^{2-}$  pair distribution functions in the  $\text{GeO}_2$  and  $1\text{Ge } 1\text{GeO}_2$  systems

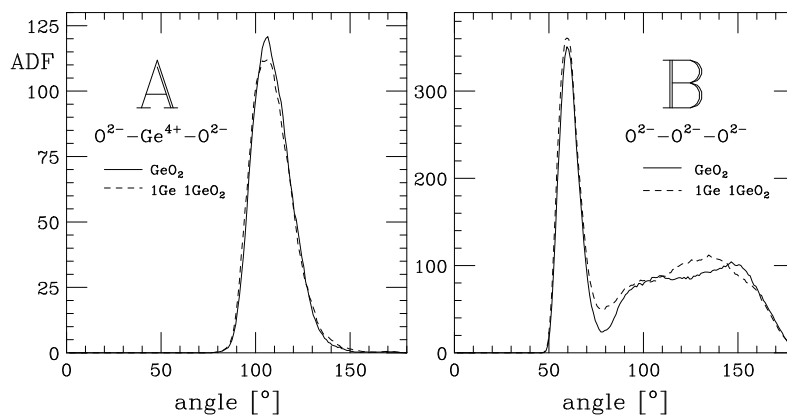


**Figure 6.** The  $\text{O}^{2-}-\text{Ge}^{4+}-\text{O}^{2-}$  and  $\text{O}^{2-}-\text{O}^{2-}-\text{O}^{2-}$  angular distribution functions in the  $\text{GeO}_2$  and  $1\text{Ge } 1\text{GeO}_2$  systems

The distributions of occurrences of the  $T_1$  and  $T_2$  values are given in Table 5. From the table results that the  $\text{Ge}^{4+}\text{O}_4^{2-}$  tetrahedra are more regular in pure  $\text{GeO}_2$  in accordance with the best fit parameters  $\sigma^2$  and  $\beta$  in distribution (1) for the  $\text{O}^{2-}-\text{O}^{2-}$  peak, Table 4.

## 5. Medium range order in the $\text{GeO}_2$ subsystem

In order to characterise the medium-range order in the  $\text{GeO}_2$  subsystem in both MD-simulated samples we have performed the cation-anion ring analysis. A



**Table 5.** Occurrences [%] of various  $T_1$  and  $T_2$  values for  $\text{Ge}^{4+}\text{O}_4^{2-}$  structural units in subsequent bins of width 0.02 in the  $\text{GeO}_2$ , and 1Ge 1GeO<sub>2</sub> systems

$T_1/T_2$ range	$\text{GeO}_2$	1Ge 1GeO <sub>2</sub>
0.00–0.02	54.1% / 48.4%	50.7% / 44.8%
0.02–0.04	34.1% / 37.8%	36.8% / 40.4%
0.04–0.06	9.4% / 11.0%	8.7% / 10.6%
0.06–0.08	1.4% / 1.4%	2.1% / 2.7%
0.08–0.10	1.0% / 1.4%	1.2% / 0.5%
0.10–0.12	– / –	0.2% / 0.5%
0.12–0.14	– / –	0.3% / 0.5%

close chain of anions and cations is called a ring. The ring containing  $N$  anions and  $N$  cations is called an  $N$ -member ring or a ring of length  $N$  [29, 30]. We have determined the smallest set of the smallest linearly independent rings, *i.e.* the basis that spans the whole set of chemically bonded germanium and oxygen atoms.

Let us discuss in brief the length distributions of the basal  $\text{Ge}^{4+}\text{-O}^{2-}\text{-Ge}^{4+}\text{-O}^{2-}\text{-}\dots$  rings (Table 6). In both systems the 5-member rings are dominating. In unreduced glass,  $\text{GeO}_2$ , only a marginal fraction of 2-member germanium-oxygen rings, corresponding to edge sharing  $\text{Ge}^{4+}\text{O}_4^{2-}$  tetrahedra, appear. However in reduced glass, 1Ge 1GeO<sub>2</sub> the edge sharing tetrahedra are more frequent. Moreover, the percentage of longer rings is lower in the reduced sample. This means that in reduced system the germania phase is more compact, in agreement with the increase of the average  $\text{Ge}^{4+}\text{-O}^{2-}$  and  $\text{O}^{2-}\text{-O}^{2-}$  co-ordination numbers due to the reduction (see Tables 3 and 4).

**Table 6.** Ge–O–Ge–O–... ring length distribution in  $\text{GeO}_2$  and 1Ge 1GeO<sub>2</sub> systems

Ring length	3	4	5	6	7
$\text{GeO}_2$	0.8%	11.6%	33.1%	37.7%	16.4%
1Ge 1GeO <sub>2</sub>	4.2%	25.5%	32.9%	27.9%	8.8%

## 6. Concluding remarks

In this contribution we describe the results of the molecular dynamics simulation of partially reduced germania of composition 1Ge 1GeO<sub>2</sub>. The clustering behaviour of neutral germanium atoms observed in our simulations agrees with experimental findings. In general, the agglomeration tendency of  $\text{Ge}^0$  atoms in  $\text{GeO}_2$  matrix is similar as in the case of heavy metal neutral atoms.

The structure of  $\text{GeO}_2$  subsystem in reduced germania, 1Ge 1GeO<sub>2</sub>, as compared with the structure of unreduced glass,  $\text{GeO}_2$ , is more complicated and the  $\text{Ge}^{4+}\text{O}_4^{2-}$  tetrahedra network is more strained. Moreover, on reduction the  $\text{Ge}^{4+}\text{O}_4^{2-}$  structural units become more irregular.

### Acknowledgements

The authors would like to thank their colleague J. Rybicki for helpful comments and suggestions.



The simulations have been performed at the TASK Computer Centre (Gdansk, Poland). The work has been partially sponsored by KBN, grant No 7 T08D 009 20.

### References

- [1] Pan Z, Henderson D O and Morgan S H 1994 *J. Non-Cryst. Solids* **171** 134
- [2] Gzowski O, Murawski L and Trzebiatowski K 1982 *J. Phys. D: Appl. Phys.* **15** 1097
- [3] Trzebiatowski K, Witkowska A and Murawski L 1999 *Mol. Phys. Rep.* **27** 115
- [4] Czajka R, Trzebiatowski K, Polewska W, Kościelna B, Kaszczyszyn S and Susła B 1997 *Vacuum* **48** 213
- [5] Rybicka A, Chybicki M and Alda W 1998 *Ceramics* **57** 135
- [6] Trzebiatowski K, Murawski L, Kościelna B, Chybicki M, Gzowski O and Davoli I 1997 *Proc. Conf. on Fundamental of Glass Science and Technology*, Vaxjo, Sweden, pp. 725–730
- [7] Witkowska A, Rybicki J, Trzebiatowski K, Di Cicco A and Minicucci M 2000 *J. Non-Cryst. Solids* **276** 19
- [8] Witkowska A, Rybicki J and Mancini G 1998 *Ceramics* **57** 147
- [9] Witkowska A, Rybicki J, Boško J and Feliziani S 2000 *IEEE Trans.: Dielectrics and Electrical Insulation* **8** 385
- [10] Witkowska A, Rybicki J, Boško J and Feliziani S 2000 *Optica Applicata* **XXX** (4) 685
- [11] Trzebiatowski K, Witkowska A and Klimczuk T 2000 *Optica Applicata* **XXX** (4) 677
- [12] Trzebiatowski K, Kusz B, Lizak W and Witkowska A 2002 *Mol. Phys. Reports* (submitted)
- [13] Nanba T, Miyaji T, Takada J and Yasui I 1994 *J. Non-Cryst. Solids* **177** 131
- [14] Rybicka A 1999 *The Structure and Properties of Lead-silicate and Lead-germanate Glasses: a Molecular Dynamics Study*, PhD Thesis, Technical University of Gdansk, Poland (in Polish)
- [15] Allen M P and Tildesley D J 1987 *Computer Simulation of Liquids*, Clarendon, Oxford
- [16] Rapaport D C 1995 *The Art of Molecular Dynamics Simulation*, Cambridge
- [17] D'Angelo P, Di Nola A, Filipponi A, Pavel N V and Roccatano D 1994 *J. Chem. Phys.* **100** 985
- [18] Filipponi A and Di Cicco A 1995 *Phys. Rev. B* **51** 12322
- [19] Mancini G 1997 *TASK Quarterly* **1** 89
- [20] Mancini G 2002 *Comp. Phys. Commun.* (submitted)
- [21] Bergmański G, Rybicki J and Mancini G 2000 *TASK Quarterly* **4** 555
- [22] Rybicki J, Bergmański G and Mancini G 2001 *J. Non-Cryst. Solids* **293-295** 758
- [23] [www.task.gda.pl/software](http://www.task.gda.pl/software)
- [24] Lottici P P, Manzini I, Antonioli G, Gnappi G and Montenero A 1993 *J. Non-Cryst. Solids* **159** 173
- [25] Ribeiro S J, Dexpert-Ghys J, Piriou B and Mastelaro V R 1993 *J. Non-Cryst. Solids* **159** 213
- [26] Umesaki N, Brunier T M, Wright A C, Hannon A C and Sinclair R N 1995 *Physica B* **213-214** 490
- [27] Medvedev N N and Naberukhin Y I 1987 *J. Non-Cryst. Solids* **94** 402
- [28] Rybicki J, Witkowska A, Bergmański G, Boško J, Mancini G and Feliziani S 2001 *Comput. Meth. Sci. Tech.* **7** (1) 91
- [29] Elliott R 1995 *J. Non-Cryst. Solids* **182** 1
- [30] Hamann D R 1997 *Phys. Rev. B* **55** 14784

